Journal of Power Sources 196 (2011) 3836–3840

Contents lists available at ScienceDirect

Journal of Power Sources

journal homepage: www.elsevier.com/locate/jpowsour

Short communication

Optical humidity sensing, proton-conducting sol–gel glass monolith

Haibin Li*, Dongliang Jin, Qingchun Yu, Hengyong Tu

Institute of Fuel Cell, School of Mechanical Engineering, Shanghai Jiao Tong University, 800 Dong Chuan Road, Shanghai 200240, China

ARTICLE INFO

Article history:
Received 12 October 2010
Received in revised form
21 December 2010
Accepted 4 January 2011
Available online 12 January 2011

Keywords:
Glass monolith
Sol–gel
Proton conduction
Humidity sensor
Fuel cell

ABSTRACT

An integrated, crack-free glass monolith is prepared via a modified sol–gel approach. It has an accessible network of channels consisting of anisotropic pores of widths ca. 20–50 nm and lengths ca. 100–250 nm. The glass monolith exhibits a transparency change based on humidity, which is utilized as a basis for optical humidity measurements. On the other hand, the glass monolith shows high proton conduction in humid atmosphere, and its proton conductivity reaches a value of 0.12 S cm^{-1} at 30 °C and 80% relative humidity.

1. Introduction

Sol–gel porous glasses and ceramics with proton-conducting properties have been have attracted great interest because of their applications in various chemical devices, such as fuel cells and sensors [1–4]. Their favorable attributes include high dimensional stability, low manufacturing costs and superior properties at both low and intermediate operating temperatures [5–8]. It is well known that the mechanism of proton conduction in porous glasses and ceramics involves the migration of protons following their dissociation from hydroxyl groups on the pore surface, and proton hopping between hydroxyl groups and water molecules [9]. The incorporation of a phosphorus component has been found to be helpful for promoting proton dissociation from hydroxyl groups, and for enhancing proton migration, due to its high cation-exchange capacity and surface acidity [10–12].

On the other hand, humidity control and monitoring are essential for applications concerning the living environment, agriculture, medicine, and the semiconductor industry [13]. Depending on the need, humidity sensing has been carried out by different kinds of sensors, such as those based on resistance [14,15], capacitance [15], or optical properties [16]. Compared with resistance- or capacitance-based humidity sensors, optical sensors have some inherent advantages, such as immunity to electromagnetic noise, the possibility of real-time monitoring, and remote sensing. These features make optical sensors powerful tools for the detection of humidity. Accordingly, there is an ever-increasing need to develop cheap and highly sensitive optical humidity sensors.

Sol–gel porous glasses and ceramics have a large surface-to-volume ratio, which allows highly sensitive detection of surface alterations caused by the adsorption/desorption of water vapor. For sol–gel porous materials, while many efforts have been directed towards the development of humidity sensors based on electrical properties [15,17,18], there have only been a few reports concerning the optical detection of humidity [19].

We report herein a glass monolith derived from tetraethoxysilane (TEOS) and orthophosphoric acid (H_3PO_4) through a hydrothermal assisted sol–gel approach. The glass monolith not only showed high proton conductivity comparable to that of Nafion®, but also exhibited a transparency change based on humidity, which was utilized as a basis for optical humidity measurements.

2. Experimental

2.1. Preparation of the phosphosilicate glass monoliths

The glass monolith was prepared by a sol–gel method, followed by a hydrothermal process. TEOS ($Si(OC_2H_5)_4$, Sinopharm, Analytical reagent) was mixed at room temperature with deionized water and hydrochloric acid (HCl) in a molar ratio of 1:4:0.004 (TEOS:H_2O:HCl). After stirring vigorously for 30 min, the resultant mixture had become a transparent solution. Orthophosphoric acid (H_3PO_4, Sinopharm, 85 wt% aqueous solution) in a molar ratio of 2:8 (H_3PO_4:TEOS) was then added to the solution, and the mixture was stirred for 1 h. The resultant solution was transferred to a

* Corresponding author. Tel.: +86 21 34206249; fax: +86 21 34206249.
E-mail address: haibinli@sjtu.edu.cn (H. Li).

0378-7753/$ – see front matter © 2011 Elsevier B.V. All rights reserved.
doi:10.1016/j.jpowsour.2011.01.004

vessel with a cover, and was aged for 3 days at room temperature to form a wetgel. The vessel with wetgel was introduced into a drying box, which was no airtight and was connected with atmosphere at a pressure of 1 atm. During hydrothermal treatment, the temperature of the drying box was keeping at 150 °C for 30 h, and a water vapor atmosphere was maintained within the drying box by providing an excess of deionized water. After these procedures, a glass monolith was obtained.

2.2. Characterization of the phosphosilicate glass monoliths

The monolith sample was photographed using a digital camera (DSC-W50, Sony). An infrared spectrum was recorded on an FTIR spectrometer (EQUINOX 55, Bruker) in transmission mode. X-ray diffraction (XRD) patterns were recorded on an X-ray polycrystalline diffractometer (D8-Advance, Bruker). The morphology of the monolith was observed by means of a field-emission scanning electron microscope (FE-SEM) (JSM-7401F, JEOL). A visible spectrometer (723PC, Cany) was used to determine the transparency of the sample, whereby the transmitted optical signal was measured over the spectral range 400–1000 nm. An environment chamber equipped with a humidity sensor (DB120, Sensirion) having sensing accuracy of 1.8% RH as reference was used to measure the spectra under conditions of controlled humidity. The electrical properties of the sample were measured using an impedance analyzer (SI-1260, Solartron). Parallel gold electrodes were sputtered onto the glass monolith through a shadow mask with two slots in size of 0.5 cm × 0.2 cm and separation of 0.5 cm. Data were collected following stepwise changes in the relative humidity. The resistance of the sample was determined from the semi-circle response on the real axis of the complex impedance plot. The proton conductivity, σ (S cm^{-1}), of the sample was calculated according to the following formula:

$$\sigma = \frac{l}{AR} \quad (1)$$

where l is the distance between the two parallel electrodes (0.5 cm), A is electrode length (0.5 cm) × membrane thickness, and R is the sample resistance.

2.3. Membrane electrode assembly (MEA) and H_2/air fuel cell test

The catalyst ink was prepared by the mixing of a Nafion® solution (5 wt% solution, Aldrich), Pt/C (60 wt% Pt/C, Johnson Matthey), Propanol with a weight ratio of 0.5:1:6. The electrodes were then prepared by spraying the catalyst ink onto the wet-proofed Toray carbon paper. The Pt loading used for the electrodes was 1 mg cm^{-2}. After that, the MEA was made by attaching the electrodes onto the glass membrane using Nafion® solution (10 wt% solution, Aldrich) as an adhesive. The active surface area of the MEA used for the fuel cell test was 0.5 cm^2. The H_2/air fuel cell was fuelled with pure hydrogen supplied onto the anode and air onto the cathode at 1 atm. The gas flow and humidification were controlled by a fuel cell testing system (CHINO, Japan).

3. Results and discussion

3.1. Morphology and structure of phosphosilicate glass monolith

The glass monolith was prepared by a hydrothermal-assisted sol–gel method. Fig. 1 illustrates photographs of the sample. They show an integrated and crack-free monolith of diameter 40 mm. Its thickness was measured as about 0.5 mm. The glass monolith was consolidated through the hydrothermal treatment. In the hydrothermal process at 150 °C used here, water vapor is introduced, which accelerates the hydrolysis of unhydrolyzed ethoxy groups of the wetgel. Subsequently, the dehydration condensation reaction leads to the formation of a silica network structure, giving rise to improved mechanical strength of the monolith. Of particular interest is the fact that the transparency of the glass monolith proved to be highly sensitive to ambient moisture. The sample was transparent at 80% relative humidity (RH) (Fig. 1a), but decreasing the humidity altered its transparency and it became opaque at 30% RH (Fig. 1b). This transparency change could be repeated by alternate exposure to dry and humid atmospheres. Thus, the glass monolith was shown to be a self-indicator of high or low humidity. On the other hand, the humidity-sensitive transparency change of the glass monolith implied that it contained interconnected pore channels, through which water molecules from ambient moisture could enter its interior.

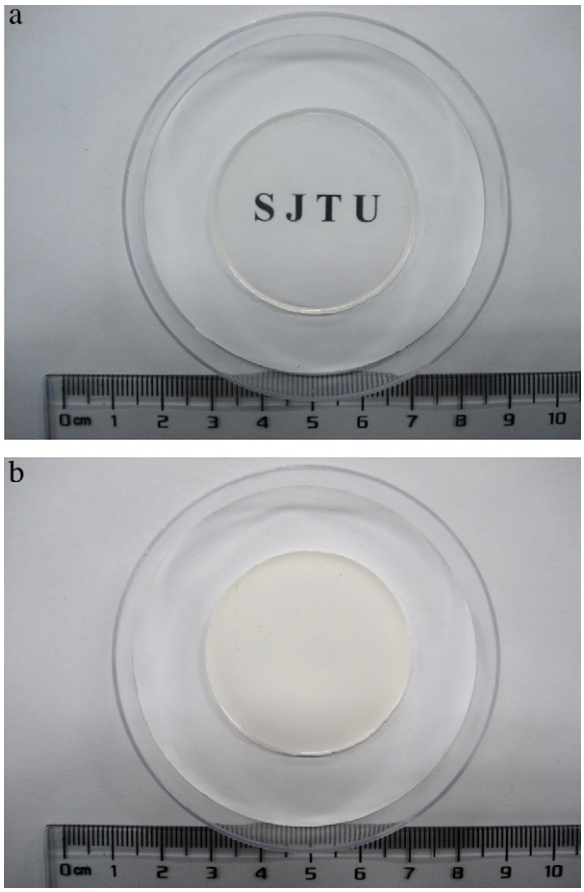

Fig. 1. Optical images at a high humidity of 80% RH (a) and a low humidity of 30% RH (b) of the glass monolith.

The IR spectrum of the glass monolith after hydrothermal treatment is illustrated in Fig. 2. The peaks at 800 and 1053 cm^{-1} can be attributed to symmetric and asymmetric stretches of the Si–O–Si unit, respectively [20]. An absorption shoulder at 960 cm^{-1} arises from the Si–O stretch of silanol groups, Si–OH [21]. The band at 890 cm^{-1} is attributed to asymmetric stretching mode of P–O–P bond, and both shoulders at 1008 and 1160 cm^{-1} are ascribed to the TO and LO modes of asymmetric stretching of Si–O–P bond, respectively [22]. An absorption peak at 1630 cm^{-1} can be assigned to the bending mode of adsorbed water molecules, H–O–H [23]. A broad absorption band appearing at 3360 cm^{-1} can be attributed to the stretching vibrations of Si–O–H and P–O–H involved in hydrogen bonding with adsorbed water molecules, H–O–H [24]. Fig. 3 shows the XRD pattern of the glass monolith. A typical amorphous reflection peak ranging from 25 to 35° is observed, suggesting the existence of an amorphous silica matrix in the sample. In addition,

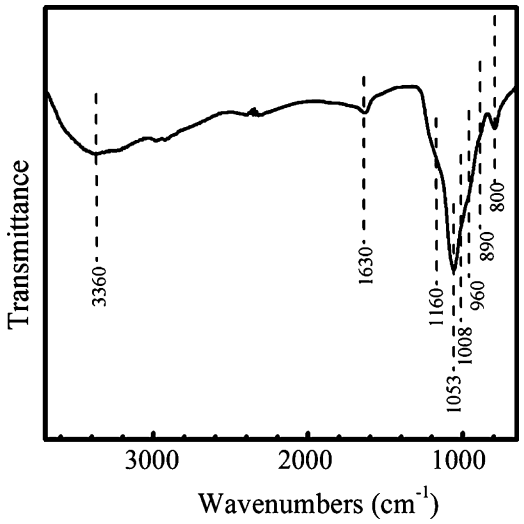

Fig. 2. Infrared spectrum of the glass monolith.

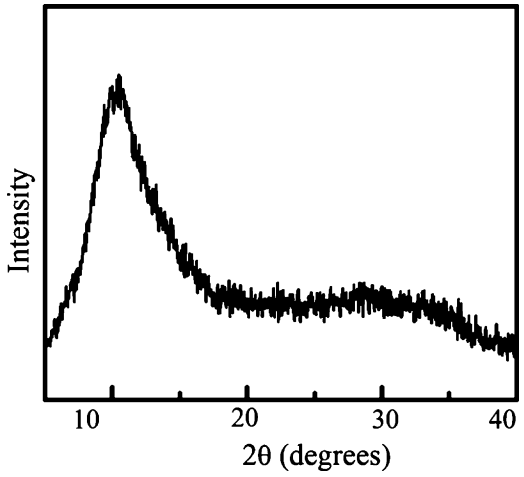

Fig. 3. XRD pattern of the glass monolith.

another reflection peak at 10.7° may be ascribed to the H_3PO_4 phase (JCPDS, 831026) introduced as a starting material.

The FE-SEM image in Fig. 4 shows the morphology of the glass monolith. It reveals that many worm-like pores were embedded uniformly in the monolith matrix. They have an anisotropic channel structure, with widths of ca. 20–50 nm and lengths of ca. 100–250 nm. The interconnected worm-like pore structure has open pores at the monolith surface, which provide access for water molecules from the external surroundings.

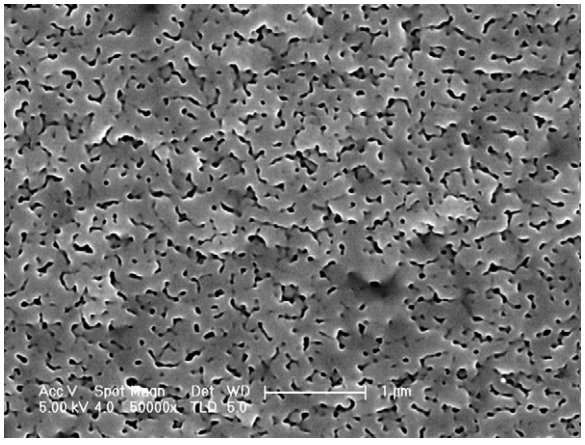

Fig. 4. FE-SEM image of the glass monolith.

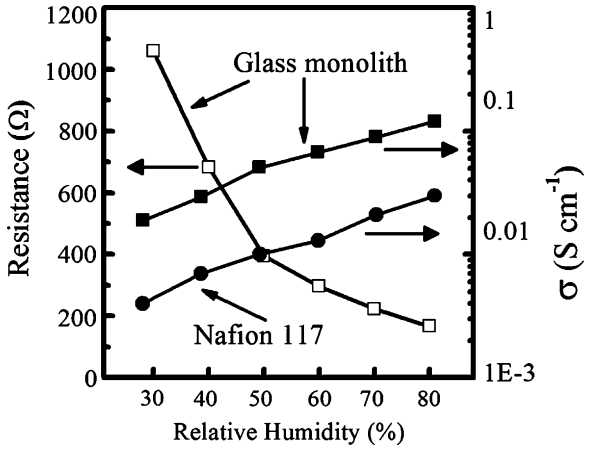

Fig. 5. Relative humidity dependences of the resistance and proton conductivity of the glass monolith measured at 30 °C. The proton conductivity of the Nafion® 117 membrane is included for comparison [25].

3.2. Proton conduction of the glass monolith and construction of a fuel cell

Fig. 5 shows the resistance and proton conductivity of the glass monolith plotted against relative humidity at 30 °C. It can be seen that the resistance of the glass monolith decreases quickly on going from 30 to 50% RH and then decreases slowly up to 80% RH, while its conductivity correspondingly shows the reverse change. The conductivity reaches 0.12 S cm^{-1} at 30 °C and 80% RH. In addition, it can be seen that the proton conductivities of the glass monolith in the measured humidity range from 30% to 80% RH are higher by one order of magnitude than those of the commercial Nafion® 117 membrane that is widely used in conventional fuel cells [25]. These results reveal that water is critically important for carrier transport in the glass monolith. For water-cooperative proton conduction, the proton dissociates from the hydroxyl group (Si–OH or P–OH) to form $H_9O_4^+$ or $H_5O_2^+$ cluster ions with adsorbed molecular water, and migrates by hopping among neighboring water cluster sites [10,26]. Compared to the SiOH bond, the POH bond of H_3PO_4 groups has higher ionic character, as a result of which it has higher cation-exchange capacity and water affinity [11]. Hence, the incorporation of H_3PO_4 groups helps to promote the dissociation and migration of protons, thereby enhancing proton conduction. The presence of H_3PO_4 groups within the glass monolith was confirmed by XRD, as shown in Fig. 3, and they are likely to be exposed to the space of the internal pores, allowing interaction with adsorbed water molecules within the pores. It is suggested that the surfaces of the pores terminated with hydroxyl bonds and bearing H_3PO_4 groups have a great affinity for water and are able to absorb water molecules into the interior to favor proton transportation. Thus, the worm-like pores in the glass monolith would serve as proton-migration channels. At lower RH, water forms a layer of clusters along the walls of the interconnected pores, while at higher RH new water molecules start filling the remaining pore space through capillary condensation [12].

The H_2/air fuel cell test was carried out with humidified H_2 and air fed into anode and cathode respectively. The gas flow rates of H_2 and air were 20 sccm and 100 sccm respectively. The open circuit voltage of the fuel cell was maintained at 0.86 V after a period of constant fuel supplement and cyclic activation. Polariza-

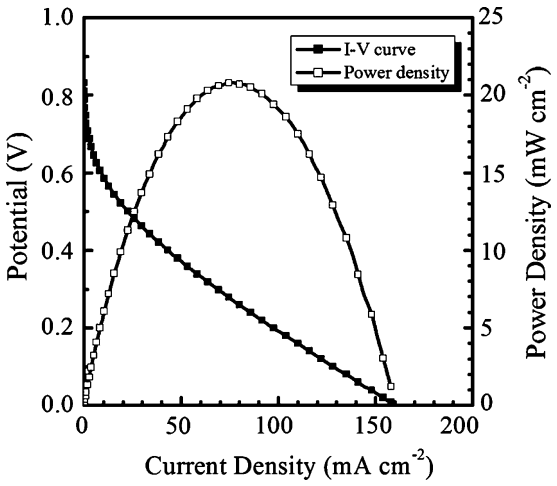

Fig. 6. *I–V* and power density curves of a single fuel cell based on the glass monolith at 30 °C.

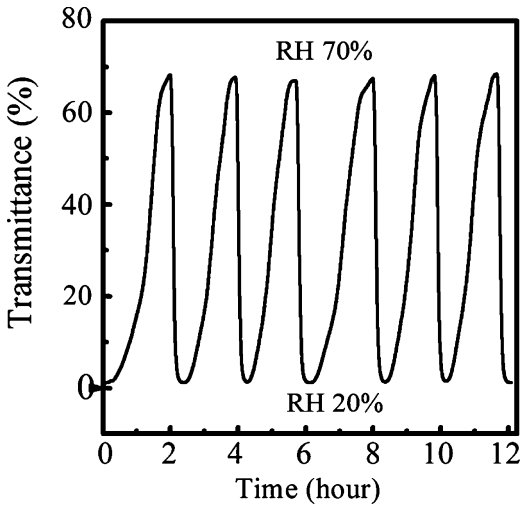

Fig. 8. The variation of the time-dependent transmittance (1000 nm, 30 °C) as the humidity alternates between 20% and 70% for multiple cycles (6 cycles).

tion curve was then recorded to show the overall performance of the fuel cell, as shown in Fig. 6. Power density was simultaneously derived from the *I–V* curve. A drop of the cell voltage even under a initial small load current shows a great activation potential loss which can be frequently observed at low operating temperatures. The obtained peak power density was 20.8 mW cm^{-2}. Area-specific resistivity (ASR) of the proton exchange membrane (PEM) is more important than proton conductivity itself in evaluating the practical performance of fuel cells. ASR value is given by t/σ, where t is the film thickness and σ is the conductivity. The glass monolith equipped in the fuel cell has a thickness of ca. 0.05 cm. By using the proton conductivity of 0.12 S cm^{-1} under 80% RH at 30 °C and the thickness of 0.05 cm, the expected ASR value of electrolyte part is 0.42 Ω cm^2. It is fairly smaller than the measured value of 3.25 Ω cm^2, which was determined by the plot in Fig. 6. Additional resistances should be due to slow charge transfer resistances through the electrodes and various contact resistances. The charge transfer resistances are associated with the thickness and configuration of catalyst layers. The sol–gel derived glass monolith is inflexible. The glass monolith could resist a certain pressure to be pressed into the membrane–electrode assembly (MEA). However, the pressure is still no enough to ensure a good adherence between glass electrolyte and electrode, resulting in quite large contact resistances.

3.3. Optical humidity sensing properties of the glass monolith

Fig. 7a shows the transmittance spectra of the glass monolith in the wavelength range 400–1000 nm under various humid atmospheres at a constant temperature (30 °C). It can be seen that the transmittance increases with increasing humidity. There are two mechanisms by which light intensity can be attenuated by a medium: atomic absorption and scattering [27]. The intrinsic absorbance of silica-based glass is low in the visible region, so the transmission intensity is mainly attenuated by scattering effects. It is well known that the scattering intensity depends mainly on the ratio of the scattering center size to the wavelength of light, and the ratio of the refractive index of the scattering center to that of the surrounding medium [27]. In the porous glass monolith, there is a channel network consisting of worm-like pores. From FE-SEM observation, it was concluded that the width of the worm-like pores was much smaller than the wavelength of visible light, but that the pores were several hundreds of nanometers in length, comparable with the wavelength of visible light. As a result, the anisotropic pores in the glass monolith can themselves act as scattering centers and scatter visible light, rendering the glass monolith opaque. On the other hand, the refractive index of water vapor is closer to that of the silica-based matrix than to that of the air voids within the glass monolith. It is suggested that, as the humidity is increased, anisotropic pores of various sizes are in turn saturated, resulting

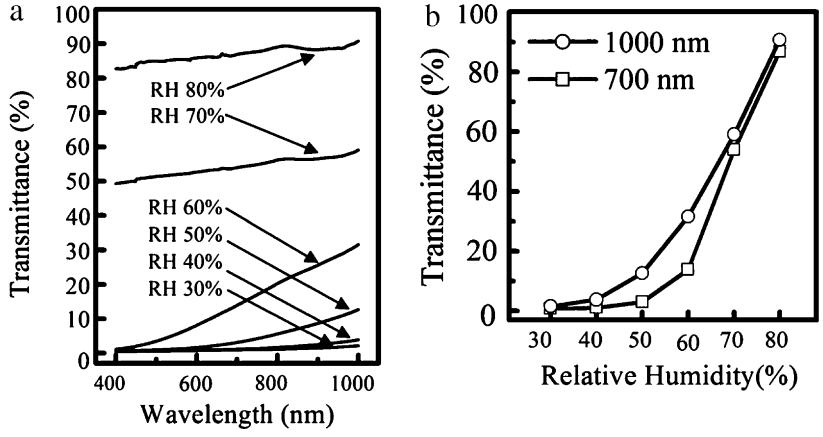

Fig. 7. (a) Transmittance spectra of the glass monolith under various humid atmospheres at 30 °C. (b) Relative humidity dependences of transmittance at wavelengths of 700 and 1000 nm.

in a decrease in the number of scattering centers due to multilayer packing of adsorbed water molecules on the pore walls, so that the transmittance of the glass monolith is enhanced.

The dependences of transmittance on relative humidity at the chosen wavelengths of 700 and 1000 nm are shown in Fig. 7b. It can be seen that the relative humidity is well reflected in the transmittance. The transmittance of both curves increases with increasing relative humidity. Specifically, the transmittance ranging from 400 to 1000 nm increases from ca. 0.35–2.1% (opaque, as seen in Fig. 1b) to ca. 82–90% (transparent, as seen in Fig. 1a) when the relative humidity is increased from 30% to 80%. This result reveals that the transparency of the glass monolith is humidity-sensitive, which we interpret in terms of a decrease of the light scattering accompanying water vapor adsorption in the pores. Thereby, with increasing humidity, the transmittance intensity of light through the glass monolith increases. In addition, the transmittance change at 1000 nm is steeper than that at 700 nm in the low-humidity region, indicating higher sensitivity. This result suggests that our humidity-sensing glass offers tunable sensitivity, and should enable convenient and cost-efficient optical humidity measurement by selecting a single wavelength.

The stability and repeatability of the glass monolith over a large RH range was demonstrated in a multi-cycle experiment in which the sample was alternately exposed to 70% RH and 20% RH atmospheres. Fig. 8 shows that as the humidity periodically alternates between 20% and 70% RH, the transmittance at the wavelength of 1000 nm switches between ca. 1.3% and ca. 68%. This response is highly reproducible. As shown in Fig. 8, the response time of the adsorption process (from 20% to 70%) for water molecules from the environment to diffuse into pores is ca. 90 min, while the desorption process (from 70% to 20%) takes ca. 30 min. This reveals that the glass monolith responds more slowly to the adsorption process than to desorption process. The glass monolith used for the response time measurement has a thickness of 0.05 cm. The response time should be dependent upon the thickness of the porous glass monolith. Thinner thickness should lead to a shorter distance for water molecules to diffuse into interior pores and consequently, shorter response time up to equilibrium would be required. The study regarding variation of the response time associated with thickness of the glass monolith is still undergoing and will be reported later.

The curves shown in Fig. 7b in which transmittances vary with relative humidity could be a calibration to measure an unknown relative humidity for a humidity sensor. In Fig. 8, the average transmittance at the wavelength of 1000 nm within 6 cycles under 70% RH accounts 67.8%. On the basis of calibration curve in Fig. 7b, the predicted relative humidity is 72.7% RH, and the error which is relative to the actual relative humidity of 70% RH measured by the humidity sensor as reference is calculated to be 3.8%.

4. Conclusion

In this study, we have demonstrated an optical humidity sensing, proton-conducting glass monolith. The glass monolith was prepared via sol–gel synthesis followed by a hydrothermal treatment. It showed the high proton conductivity which can exceed 0.1 S cm^{-1}. The transparency of the glass monolith with porous structure has been found to be changed based on environmental humidity. This optical humidity sensing glass should be applicable for the development of a novel humidity sensor. In addition, because of its high proton conduction in combination with its capability of optical monitoring of humidity, our glass monolith is expected to be promising for use as an electrolyte in fuel cells that are required to operate under conditions of controlled humidity.

Acknowledgements

This work was supported by the International Science and Technology Cooperation Program (Grant 2008DFA51200) and the National High-Tech R&D Program (863 Program) (Grant 2009AA05Z113) of Ministry of Science and Technology of China, National Natural Science Foundation of China (NSFC Grant 50672058), and the Shanghai Pujiang Program (Grant 08PJ1406500).

References

[1] M. Nogami, H. Matsushita, Y. Goto, T. Kasuga, Adv. Mater. 12 (2000) 1370–1372.
[2] M.T. Colomer, F. Rubio, J.R. Jurado, J. Power Sources 167 (2007) 53–57.
[3] F. Jiang, Z. Di, H. Li, H. Tu, Q. Yu, J. Power Sources 196 (2011) 1048–1054.
[4] M. Nogami, M. Matsumura, Y. Daiko, Sens. Actuators B 120 (2006) 266–269.
[5] Y. Daiko, T. Akai, T. Kasuga, M. Nogami, J. Ceram. Soc. Jpn. 109 (2001) 815–817.
[6] Y. Parka, M. Nagai, J. Kim, K. Kobayashi, J. Power Sources 137 (2004) 175–182.
[7] S. Suzuki, Y. Nozaki, T. Okumura, M. Miyayama, J. Ceram. Soc. Jpn. 114 (2006) 303–307.
[8] C. Sun, U. Stimming, Electrochim. Acta 53 (2008) 6417–6422.
[9] M. Nogami, R. Nagao, C. Wong, J. Phys. Chem. B 102 (1998) 5772–15772.
[10] M. Nogami, R. Nagao, C. Wong, T. Kasuga, T. Hayakawa, J. Phys. Chem. B 103 (1999) 9468–9472.
[11] A. Bhaumik, S. Inagaki, J. Am. Chem. Soc. 123 (2001) 691–696.
[12] F.M. Vichi, M.I. Tejedor-Tejedor, M.A. Anderson, Chem. Mater. 12 (2000) 1762–1770.
[13] Z. Chen, C. Lu, Sens. Lett. 3 (2005) 274–295.
[14] L.J. Golonka, B.W. Licznerski, K. Nitsch, H. Teterycz, Meas. Sci. Technol. 8 (1997) 92–98.
[15] C.T. Wang, C.L. Wu, I.C. Chen, Y.H. Huang, Sens. Actuators B 107 (2005) 402–410.
[16] J. Shi, V.K.S. Hsiao, T.R. Walker, T.J. Huang, Sens. Actuators B 129 (2008) 391–396.
[17] A. Bearzotti, J.M. Bertolo, P. Innocenzi, P. Falcaro, E. Traversa, J. Eur. Ceram. Soc. 24 (2004) 1969–1972.
[18] P. Innocenzi, A. Martucci, M. Guglielmi, A. Bearzotti, E. Traversa, Sens. Actuators B 76 (2001) 299–303.
[19] B.C. Yadav, N.K. Pandey, A.K. Srivastava, P. Sharma, Meas. Sci. Technol. 18 (2007) 260–264.
[20] I. Vasiliu, M. Gartner, M. Anastasescu, L. Todan, L. Predoana, M. Elisa, C. Grigorescu, C. Negrila, C. Logofatu, M. Enculescu, A. Moldovan, G. Pavelescu, M. Zaharescu, Opt. Quant. Electron. 39 (2007) 511–521.
[21] H. Li, T. Kunitake, Microporous Mesoporous Mater. 97 (2006) 42–48.
[22] P. Massiot, M.A. Centeno, I. Carrizosa, J.A. Odriozola, J. Non-Cryst. Solids 292 (2001) 158–166.
[23] Y. Jin, S. Qiao, J.C.D. da Costa, B.J. Wood, B.R. Ladewig, G.Q. Lu, Adv. Funct. Mater. 17 (2007) 3304–3311.
[24] A. Aronne, M. Turco, G. Bagnasco, P. Pernice, M. Di Serio, N.J. Clayden, E. Marenna, E. Fanelli, Chem. Mater. 17 (2005) 2081–2090.
[25] Y. Sone, P. Ekdunge, D. Simonsson, J. Electrochem. Soc., 143 (4) 1254–1259.
[26] K.D. Kreuer, Chem. Mater. 8 (1996) 610–641.
[27] T. Berthier, V.M. Fokin, E.D. Zanotto, J. Non-Cryst. Solids 354 (2008) 1721–1730.